ELSEVIER

Journal of Chromatography A, 743 (1996) 57–73

JOURNAL OF CHROMATOGRAPHY A

Studies on the expansion characteristics of fluidised beds with silica-based adsorbents used in protein purification[1]

Gerard M.S. Finette, Qi-Ming Mao, Milton T.W. Hearn*

Centre for Bioprocess Technology, Department of Biochemistry and Molecular Biology, Monash University, Clayton, Victoria 3168, Australia

Abstract

In these investigations, a detailed examination of the fluid dynamic characteristics of expanded beds containing silica-based chromatographic adsorbents has been carried out. In particular, the effects of the column accessories such as distributor design and the flow-rate on the dispersion coefficient of the adsorbent particles have been examined. The experimental data have been analysed in terms of residency time effects, fluid flow characteristics and physical properties of the adsorbent particles using several different theoretical models. In common with experience of packed-bed systems, the results confirm that the optimisation of the dynamic capacities as well as the dynamic adsorption rates of adsorbents in expanded-bed systems must take into account column design characteristics as well as the physical/chemical features of the adsorbents, if the highest productivities of expanded-bed/fluidisation procedures are to be achieved with crude feedstocks from biotechnological applications.

Keywords: Adsorbents; Stationary phases, LC; Dispersion coefficients; Proteins

1. Introduction

Recently, expanded- or fluidised-beds have emerged as a very useful adjunct to packed-beds for the chromatographic capture and purification of proteins, particularly with crude feed stocks derived from fermentation processes or bulk biological fluids such as whey or blood serum fractions [1–9]. Not only do expanded-bed/fluidised systems offer the possibility of more rapid processing times, resulting in less degradation and product losses, but also the capital investment and process labour costs associated with purchase and operation of centrifugation and/or ultrafiltration equipment can be considerably reduced, thus improving the overall economics and productivity of the recovery and purification process. The design features of the fluidised column can be anticipated to represent a very important aspect if uniform fluidisation is to be achieved. Incorrect design of the distributor could, for example, result in channelling and lead to an impaired estimation of the adsorption kinetics. The involvement of uniform fluidisation can be characterised from studies on the fluid flow dynamics inside the column. Most studies on solid–liquid mixing with particulate fluidised beds have been realised by fluidising transparent or colourless solid particles in a liquid and by following the motion of opaque tracer particles [10–16]. The electrical conductivity method has also been used to determine the degree of mixing [16–20].

In order to characterise the expanded-bed behav-

*Corresponding author.

[1]Part CLIX of the series High-performance liquid chromatography of amino acids, peptides and proteins. For Part CLVIII see reference [71].

0021-9673/96/$15.00
PII S0021-9673(96)00321-4

iour of a range of silica- and zirconia-based ion-exchange adsorbents as part of our on-going investigations on the adsorption behaviour and subsequent selective desorption from expanded-/fluidised beds of proteins present in complex feedstocks, the bed expansion characteristics, minimum fluidisation and terminal velocities, and dispersion coefficients of several silica-based preparative adsorbents of different particle sizes have been investigated and compared to a polymeric adsorbent of comparable physical characteristics. The results confirm that the particle size and particle density play critical roles in determining the minimum and terminal fluid velocities, whilst the influence of column accessories directly impact on the pressure drop characteristics of the system and mixing properties.

2. Materials and methods

2.1. Materials

Human serum albumin (HSA), as a 20% (w/v) solution was generously provided by the Commonwealth Serum Laboratories (CSL) (Melbourne, Australia). The porous silica particles which included LiChroprep DIOL (25–40 and 40–63 μm) and Fractosil Si1000 (63–100 μm) were a gift from E. Merck (Darmstadt, Germany). The soft resin, Fractogel HW55, was obtained from Sigma (St. Louis, MO, USA).

2.2. Preparation of buffers

For the determination of the mixing properties, the elution buffer consisted of 0.15 *M* sodium acetate buffer, pH 4.5. This buffer was prepared by mixing glacial acetic acid (BDH, Melbourne, Australia) with distilled water and the pH was adjusted by adding sodium hydroxide. For all desorption steps, fresh buffers were made daily with degassed Milli-Q water, and filtered through a sterile 0.45-μm Millipore filter.

2.3. Preparation of proteins

The stock solution of HSA was divided into 1 ml aliquots and kept refrigerated at −20°C. When experiments were performed using HSA (20%, w/v) as a model protein, the 1 ml aliquots were diluted in elution buffer solution and made up to the appropriate concentration. The extinction coefficient was measured spectrophotometrically and found to be equal to 0.583 for a HSA protein concentration of 1 mg/ml.

2.4. Measurement of response parameters

For experiments performed in fluidised columns, the apparatus consisted of a column with a 1-cm internal diameter and 15 cm maximum height that was made of polycarbonate material. The column with variable endfittings was designed by the investigators as part of this study at the Centre for Bioprocess Technology, Monash University, and made in the workshop of the Chemical Engineering Department. The column was connected to a high flow-rate peristaltic pump (model 503U) purchased from Watson and Marlow (Melbourne, Australia). In the fluidised column, the channelling effect was minimised by the addition of glass beads (250 μm) purchased from Selby Scientific (Melbourne, Australia), which were packed at the bottom of the column. Backflow was prevented by the use of a metallic grid (0.5 μm) placed at the very bottom of the column. A pressure gauge (VDO, Australia) was also connected to the bottom of the column. After the adsorbent particles had settled at the bottom of the column, the elution buffer (0.15 *M* sodium acetate buffer, pH 4.5) was passed through the column at a specific flow-rate. Once the bed was stabilised (no increase in bed height being registered) and the adsorbent fluidised, a plunger of novel design, also made in the workshop of the Chemical Engineering Department, Monash University, was placed just over the top of the fluidised particles to reduce the dead volume. The HSA solution, diluted in elution buffer was then passed through the column and the output response was monitored by means of a UV detector (Pharmacia Biotech, Uppsala, Sweden) connected to a two-pen chart recorder (Model 2210, from Pharmacia Biotech). A breakthrough profile similar to that obtained from the loading of a protein solution of different concentrations onto a packed column containing the adsorbent was generated. The dispersion coefficients

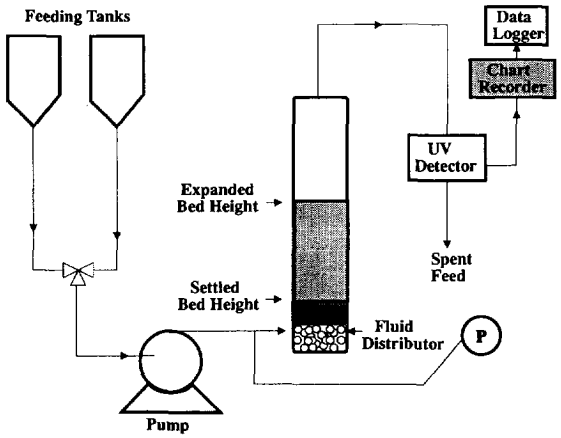

Fig. 1. Schematic representation of the fluidised bed system.

were then determined by fitting the predicted breakthrough profiles obtained from the axial dispersion model [21] and the tanks in series model [22–26] to the experimental breakthrough profiles.

Prior to the determination of the dispersion coefficient, the bed expansion characteristics were also determined. A known amount of adsorbent was packed into the column and the bed was allowed to stabilise. Once settled, the bed height was registered. Elution buffer (0.15 *M* sodium acetate buffer, pH 4.5) was then passed through the column at different flow-rates. While carrying out the bed expansion experiments, the minimum fluidising velocity was determined, i.e. the minimum fluidising velocity to cause the bed to be in the loosest form of packing. The value of the minimum fluidising velocity was determined by the pressure drop method [27–31]. A pressure gauge was connected on the fluid line to measure the system pressure drop, as shown in the schemata of the equipment layout (Fig. 1). In circumstances where it proved difficult to measure the minimum fluidising velocity, correlations obtained from literature were used to derive this value.

3. Results and discussion

3.1. Theoretical background

Dispersion of fluid in a fluidised bed is composed of contributions from molecular longitudinal and axial diffusion, turbulent diffusion and convective diffusion caused by a non-uniform velocity distribution. It has been observed [15] that the dispersion coefficients of fluid are independent of the diffusivity of the tracer particle used to characterise the degree of mixing in the expanded/fluidised bed. Previous studies [18,32–38], mainly from chemical engineering applications, have shown that the longitudinal dispersion for fluid in a solid–liquid fluidised column can be determined from the following dimensionless terms

$$X = \frac{d_p U_o D}{U d_p \rho_f / \nu} \quad (1)$$

where d_p = particle diameter (m), U_o = interstitial velocity (ms^{-1}), U = superficial velocity (ms^{-1}), D = dispersion coefficient (m^2s), ρ_f = fluid density (kg m^{-3}) and ν = viscosity of fluid (kg m^{-1} s).

The term X is the ratio of the Peclet number over the Reynolds number, i.e. $X = P_e/R_e$. In previous studies related to the validation of Eq. (1), a range of different materials was used in expanded/fluidised bed columns for the determination of the dispersion coefficients, including glass [17,33,38,39], sand [40,41], lead [39,42], polystyrene [15–17] and polypropylene [16]. Collectively, these studies have shown that the longitudinal dispersion coefficient is affected by many factors, with the density and concentration of the particles included amongst those parameters known to affect the axial dispersion coefficient [39].

Several groups of investigators have also observed that the ratio of particle-to-column diameter affects the dispersion coefficient to varying extents. Stayanovskii [43], for example, found that the dispersion coefficient was inversely proportional to the column diameter, whereas an increase in axial mixing with increasing column diameter has been observed by some investigators [44–46]. However, other investigators could not observe any change in the dispersion coefficient in studies examining the effect of the ratio of particle diameter to column diameter on the dispersion coefficient [17,32,41,47]. For example, in the studies of Kikuchi et al. [17] and van der Meer et al. [47], columns with diameters ranging from 2 to 6 cm were examined to study the effect of column diameter on the dispersion coeffi-

cient, paralleling the use of column types that are employed in process-scale high-performance chromatographic separations. In addition, Cairns and Praunitz [39] observed that particle agglomeration can also affect the axial dispersion. With fluidised lead and glass beads in water, the axial dispersion coefficient for lead in water was found for example to be twice that of the glass–water system, consistent with the observation that the lead–water system has a greater tendency to aggregate [27].

The effect of particle size and column bed height on the dispersion coefficient has also been studied by various investigators. In these studies, the dispersion coefficient was generally found to be lower for smaller particles [17,19,48–50]. With most systems, the dispersion coefficient was not affected by change in the bed height [15,19,24,35,39]. However, Krishnaswamy et al. [37] have proposed a correlation whereby the dispersion coefficient was dependent on bed height. With spherical and irregular particles fluidised in columns of different dimensions, conflicting observations have been made concerning the effect of flow-rate on the dispersion coefficient. In some studies, the dispersion coefficient was found to continuously increase as the flow-rate was increased [32,41,50,51], whilst in other investigations, the dispersion coefficient was found to reach a maximum as the flow-rate was increased [11,12,17,39]. In these latter investigations, a maximum dispersion coefficient was observed when the bed voidage ranged from 0.7–0.8.

It has been suggested [24] that an increase in bed voidage at higher velocity resulting in a reduction in the number of particles occupying the same volume, causes a reduction in the dispersion coefficient. El-Temtamy et al. [52], working with glass beads with average diameters of 0.45, 0.96, 2 and 3 mm, observed different mixing behaviours with increasing fluid velocity. The axial dispersion of the smallest particle size (0.45 mm) was reduced with an increase in liquid velocity, reached an asymptotic value with 0.96 mm particle beads and passed through a maximum value with beads of 2 mm particles. An increase in the dispersion coefficient with liquid velocity similar to that observed with 0.96 and 2 mm particle beads was noted by Kim et al. [53] who used 2.5 mm irregular gravel and 6 mm glass ballotini in a three-phase fluidised bed. Mehta and Shemilt [38], working with 0.5 mm glass beads, observed a maxima at $\epsilon = 0.65$, followed by a minima at $\epsilon = 0.70$–0.75, after which the axial dispersion increased again up to $\epsilon = 0.90$, then decreased again depending on the viscosity of the liquid.

Tang and Fan [19] did not observe any maxima in the dispersion coefficient with particles of average diameter between 1.0–2.5 mm and a density ranging from 1.1–1.3 g cm^{-1}. On the other hand, these investigators observed a maximum in the energy dissipation rate per unit liquid mass for all particles at a bed voidage equal to 0.7 and related this phenomenon to the wake dispersion effects that are formed on top of particles and which are assumed to contain highly mixed zones of fluid which multiply with increasing flow-rate. An increase in fluid velocity will cause bubble dispersion, lowering the particle concentration and increasing the particle oscillations. The formation of finer bubbles and the lowering of particle concentration will contribute to a reduction in the axial dispersion, whereas an increase in particle oscillation will contribute to an increase in the longitudinal dispersion coefficient. The overall effect will depend on the particle characteristics [52].

Many correlations have been proposed to determine the axial dispersion coefficients in solid–liquid fluidised beds. Correlations have been proposed for systems covering a rather low Reynolds number range [40,41,54], whilst other correlations have been proposed for a wider Reynolds number range [32,36,37,55–57]. Chung and Wen [32] approximated the liquid fluidised bed by a packed-bed with a large bed fraction and proposed a correlation applicable to both fixed and fluidised beds with a 46% standard deviation, namely

$$\frac{DY}{\upsilon} = \frac{\mathrm{Re}}{[0.20 + 0.011\,\mathrm{Re}^{0.48}]} \tag{2}$$

where $Y = \mathrm{Re}_{mf}/\mathrm{Re}$ and Re_{mf} = Reynolds number at minimum fluidising velocity.

Kikuchi et al. [17], working with polystyrene and glass beads having diameters ranging from 239 to 1887 μm, found that low density solid particles have lower dispersion coefficients than denser particles and proposed the following correlation, namely

$$\frac{D}{l} = 500\Omega^{0.43} \exp(-20.5(0.75 - \epsilon)^2) \tag{3}$$

where D is the axial dispersion coefficient, l is the kinematic viscosity of liquid, Ω is the energy dissipation rate ($m^2\ s^{-3}$) and ϵ is the void fraction. However, there is disagreement in the literature concerning the values obtained from these different correlations for the axial dispersion coefficient. For example, in the systematic study of Kikuchi et al. [17], the experimental results were compared with correlations proposed by various other investigators [32,40,41,54,56], with the predicted results deduced from the correlations shown to vary between 160% to 3000% from the experimentally observed values. This large difference could be due to a range of factors affecting experimental results, including the contribution of poor distributor performance in fluidised beds which would cause severe distortion of the bed hydrodynamics [15,16,18].

Correlations for the determination of the dispersion coefficient are known to be subject to errors, particularly when the proposed correlation is dependent upon other correlations. For example, in the correlation proposed by Krishnaswamy and Shemilt [36], the effects of the particle terminal velocity, the open tube dispersion coefficient, particle density, shape of the particle and radial velocity on the liquid axial dispersion are taken into account. However, the terminal velocity and the open tube dispersion coefficient were obtained from a correlation proposed by Tichateck et al. [58] and Benarek and Klumpar [59], respectively. Thus, a 10% error made in the measurement of the terminal velocity could lead to 19.5% deviation from the true value of the dispersion coefficient [33]. Subsequent investigations have indicated that the correlations proposed by Chung and Wen [32] and Krishnaswamy and Shemilt [36] were only applicable for particles having large diameters and high densities [17,19].

Determination of the dispersion coefficient for a particular particle and column system helps to define the flow characteristics occurring inside the column. The greater mixing of the fluid inside the column which occurs in expanded or fluidised columns will affect the nature of the binding kinetics of a solute to an adsorbent. So far, protein purification has been mainly performed with the traditional packed columns where the effect of axial dispersion is negligible. Metzdorf et al. [60] have studied the dispersion coefficient in the fluidised column where silica (125–160 μm), having a density of 1.47 g cm^{-1}, was used for the adsorption of galactosidase. The dispersion coefficient was determined as a function of the bed expansion and was found to increase with increasing velocity, although the effect of the mixing characteristics of the flowing fluid on the immobilisation of the enzyme was not examined. Draeger and Chase [1–4] have also studied the dispersion coefficient of a fluidised column in which bovine serum albumin was adsorbed onto Q-Sepharose Fast Flow (44–180 μm) having a density of 1.13 g cm^{-1}. However, the adsorbent chosen had a low density and no mixing was obtained. A D/U_oL value equal to 0.007, with a D value equal to $5.2 \cdot 10^{-8}\ m^{-2}\ s^{-1}$, was reported by these investigators. In this system the flow characteristics were laminar with the particles assumed to behave in the same manner as in the packed column, where low flow-rates were applied to avoid an increase in pressure drop. Under these conditions, it can be concluded that the fluid was moving along with plug flow characteristics.

3.2. Determination of dispersion coefficients

3.2.1. Residence time distribution

The time taken for a molecule of fluid to pass from one end of the vessel to the other end is defined by the exit age distribution function (E_a) or the residence time distribution function. In a closed vessel, it is obvious that different elements of the fluid will take different paths, and will require different periods of time to pass from one end of the column to the other. As a result, the mean average time for all elements of the fluid to traverse the column can be represented by

$$\bar{t} = \frac{L}{U_o} \tag{4}$$

where U_o is the interstitial velocity and L is the column length.

The E_a of the fluid can be determined experimentally by the step function (equivalent to frontal breakthrough with a packed bed) or pulse input method (equivalent to a zonal elation profile with a packed bed). As described in the Section 2, the step function approach was followed in the present investigations. In the step function method, the curve generated, usually called an F-curve, is expressed as

the ratio of the input and output concentration ratios (C/C_o). The shape of the curve will depend on the mixing state of the system. Irrespective of the hydrodynamic or rheological circumstances which prevail in the column, the area behind the curve gives the time spent by a fluid element inside the vessel. The type of curve generated from the pulse input approach is a Gaussian function and is usually called the *C*-curve. Normalisation of the data associated with either the *F*- or the *C*-curve is usually achieved by dividing the measured concentration by the area under the concentration–time curve.

3.2.2. Models for non-ideal flow

Depending on the column and inlet distributor design, the physical and chemical characteristics of the particles, the temperature and the composition of the fluid, non-ideal flow can occur inside the column. These flow features can be characterised by a variety of different models that vary in complexity. For example, various modifications of the "one parameter model" have been employed to adequately represent the fluid flow in packed beds, whilst some models containing from two to six parameters have been employed with fluidised beds. The major focus of the present investigations involved the "one parameter model", which include the axial dispersion model (ADM) [21] and the tanks in series model (TSM) [22–26]. With both models, it was more convenient to measure the time in units of mean residence time, which is defined as the ratio of the time spent by an eluent molecule against the average time. The average time can be defined as the length of the column over the interstitial velocity (Eq. 4), which is itself the ratio of the superficial velocity against the bed voidage according to the following expression:

$$U_o = U/\epsilon \ (\mathrm{ms}^{-1}) \tag{5}$$

3.2.3. The axial dispersion model

The ADM assumes that the column can be represented by a turbulent flow reactor in which the axial dispersion can mainly be equated with the effective diffusivity D_e. Moreover, the ADM further assumes that both the concentration profile and the axial velocity (U) are uniform across the diameter of the column. According to a modification of Fick's law, the molecular diffusion can be represented in the case of expanded or fluidised beds by the following equation:

$$\frac{\delta C}{\delta t} = D\frac{\delta^2 C}{\delta \chi^2} \tag{6}$$

where D, instead of being the coefficient of molecular diffusion that characterises the process in the Fick's equation for a well-stirred tank, is here called the longitudinal or axial dispersion coefficient that characterises the degree of backmixing during the fluid flow, and χ is the characteristic length. The above basic differential equation representing the dispersion model can also be represented in the dimensionless form shown below

$$\frac{\delta C}{\delta \theta} = \left[\frac{D}{U_o L}\right] \times \left[\frac{\delta^2 \chi}{\delta z^2}\right] - \frac{\delta C}{\delta z} \tag{7}$$

where

$$\theta = \frac{t}{\bar{t}} \tag{8}$$

and

$$z = (U_o t + \chi)/L \tag{9}$$

The dimensionless term (D/U_oL), or the column dispersion number, is the inverse of the Peclet number. The equation representing the dependency of concentration on time dispersion model is shown below

$$\frac{C}{C_o} = \frac{1}{2}\left[1 - \mathrm{erf}\left[\frac{1}{2} \times \sqrt{\frac{U_o L}{D}} \times \frac{1-\theta}{\sqrt{\theta}}\right]\right] \tag{10}$$

From Eq. 10, the value of D can be iteratively derived so that the curve derived from the above equation matches the experimental curve. Two extreme cases can easily be identified from Eq. 10, namely (i) when $D/U_oL \to 0$, no axial dispersion is present in the system and the column behaves as a plug flow, and (ii) when $D/U_oL \to \infty$, an infinite diffusivity is observed in the system and a stirred tank performance is obtained.

3.2.4. The tanks in series model

The TSM is visualised as various flow regions that are connected in parallel. It assumes that there are several smaller tanks within the column that perform

the same function as the actual column. This model has been discussed by various investigators [22–26]. Since in the stirred tank model all the tanks are similar, the total mean residence time is identical for each tank and the average residence time per tank is θ/m. After the introduction of an amount of material into the system at $t=0$, the amount of material present in stages 1, 2...m can be represented by N_1, $N_2...N_m$. The final equation governing the transport is then given by

$$\frac{dN_m}{dt} = -\frac{N_m}{\tau} + \frac{N_{m-1}}{\tau} \quad (11)$$

where τ = residence time per stage.

From the solution of Eq. 11 for the m-stages, it can be shown that on continuous introduction of material from time $t=0$ onwards, the concentration profile of material leaving the column at time t is given by

$$\frac{C_m}{C_o} = J_m(\theta) = 1 - e^{-m\theta}\left[1 + m\theta + \frac{1}{2!}m\theta^2 + \cdots + \frac{1}{(m-1!)}m\theta^{m-1}\right] \quad (12)$$

Similarly, from Eq. 12, two extreme cases can be identified for the TSM, namely (i) when $m=\infty$, leading to the absence of axial diffusion and (ii) when $m=1$, leading to the formation of only one mixing stage in the entire vessel and, as a result, the dispersion number tends towards infinity. Since the dispersion number of a solvent through a column can be explained in terms of eddy diffusion, different relationships linking the number of stages, m, and the dispersion number have been proposed. For example, Kramers and Alberda [24] have proposed the following relation

$$\frac{D}{U_o L} = \frac{1}{[2(m-1)]} \quad (13)$$

whilst Klinkerberg and Sjenitzer [25] have derived the relationship linking D and m shown below

$$\frac{D}{U_o L} = \frac{1}{2m} \quad (14)$$

When m is large, i.e. when the fluid flow inside the column is close to plug flow, the dispersion numbers determined from Eqs. 13,14 are almost identical. However, when $m=1$, it can be concluded from Eq. 13 that $D/U_oL \rightarrow \infty$, whilst Eq. 14 leads to $D/U_oL = 0.5$.

3.2.5. Bed expansion characteristics

In the present series of experiments, several different silica-based adsorbents with physical characteristics appropriate for preparative application in expanded-bed/fluidised columns were examined. Representative data for the bed expansion of these different silica-based adsorbents are presented in Fig. 2a as plots of the height (H) of the fluidised column against the superficial velocity. A linear dependency was observed for H versus U_o for the different

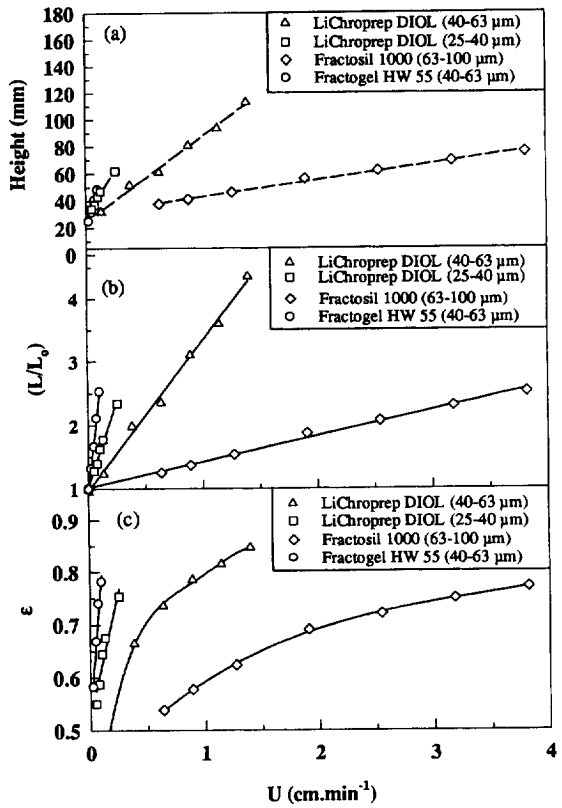

Fig. 2. Effect of flow-rate on (a) bed height, (b) ratio of bed height and (c) bed voidage for different adsorbents. In each case 2.5 g of adsorbent were placed into a column of internal diameter of 10 mm and 0.15 M sodium acetate buffer, pH 4.5, was used as the eluent.

adsorbents in the range of flow-rates studied. Among the adsorbents studied, the plot resulting from the expansion of Fractogel HW55 was the steepest, while the plot resulting from the expansion of Fractosil 1000 was the shallowest. Moreover, these data indicated that when the same superficial velocity was applied, the bed voidage observed for the Fractogel particles was the largest, whereas the bed voidage with the Fractosil particles was the lowest. The densities of these adsorbents were measured by the displacement method, where it was found that Fractogel HW55 (1.06 g cm^{-3}) has the lower density compared to Fractosil 1000 (1.35 g cm^{-3}). From these results, it can also be concluded that the respective expansion in bed height for the different particles at the same flow-rate is proportional to the density and particle size.

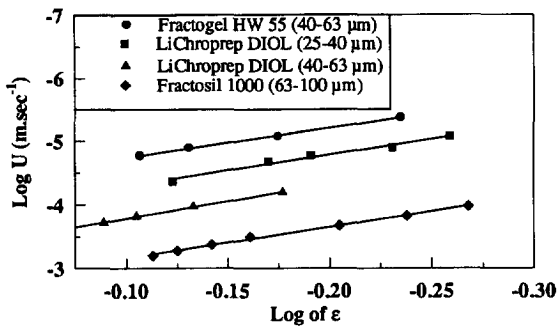

Fig. 3. Plot of the logarithm of the bed voidage versus the logarithm of the superficial velocity for different adsorbents. The column dimensions and eluent composition are given in the legend to Fig. 2.

The effect of the particle size was also examined when LiChroprep DIOL of two different mean particle diameter ranges (25–40 and 40–63 μm) were allowed to expand at a particular velocity. Fig. 2a shows that the plot resulting from the expansion of LiChroprep DIOL (25–40 μm) was steeper than that resulting from LiChroprep DIOL (40–63 μm). In fact, the different extents by which these two adsorbents expanded at a particular linear velocity varied by a factor of 1.5. The ratio of the expanded bed height to bed height at rest (L/L_o) was also plotted against the superficial velocity and the results are shown in Fig. 2b, where essentially linear dependencies were observed.

Fig. 3 shows the bed expansion characteristics of the different adsorbents fluidised with a 150 m*M* sodium acetate buffer, pH 4.5, in terms of the dependency of superficial velocity versus bed voidage employing the approach of log U_o versus log ϵ as proposed by Richardson and Zaki [61] and Richardson and Meikle [62]. In particular, the slope of the plot of the logarithm of the superficial velocity versus the logarithm of the bed voidage gives the value of the n index and the y-intercept gives the terminal velocity. Table 1 compares the n-index values obtained for the four different adsorbents with those predicted by the Richardson-Zaki correlation. As evident from these results, the n-index values were within the range of values predicted from the Richardson-Zaki correlation. For example, values of the n-index equal to 4.65 and 4.89 were obtained for Fractogel HW55 and Fractosil 1000, respectively, compared to an n-index value of 4.65 predicted for particles with average diameters <100 μm by the Richardson-Zaki correlation. The results also indicate that the n-index value increased with the particle size, i.e. the n index for LiChroprep DIOL (25–40 μm) was 4.9 compared to 5.28 for LiChroprep DIOL (40–63 μm). This increase in the value of the n-index for the larger particles is consistent with the correlation proposed by Richardson and Zaki [61], where the n-index is dependent on the ratio of particle diameter to column diameter. However, as evident from our experimental results, the data obtained from the bed expansions of LiChroprep DIOL were higher than the n-index values obtained from the Richardson-Zaki correlation, if an n-index value of 4.8 was used as the Richardson-Zaki parameter for spherical particles in a laminar flow regime [62,63]. The higher n-index value obtained from the expansion of LiChroprep DIOL particles (40–63 μm) at different linear flow-rates may thus be due to the fact that the particles were angular. Higher values of the n-index than predicted from the Richardson-Zaki correlation have been previously obtained [64]. A decrease in the value of the n index with larger particle size should not be surprising, if it is assumed [65] that there is a greater proportion of occluded liquid with particles of smaller size.

3.2.6. Determination of the minimum fluidising velocity

Table 2 shows the minimum fluidising velocity of the different adsorbents. Because of the design of the

Table 1
Determination of the expansion index using the correlation proposed by Richardson and Zaki [61]

	Particle range (μm)	Mean diameter (μm)	Shape	n-index
Richardson and Zaki [61]	–	>100	Spherical	4.65
Richardson and Meikle [62]		<100	Spherical	4.79
		5.5		10.5
Jottrand [69]	–	20.2	Angular	5.60
		28.7	Angular	5.60
		43.1	Angular	5.60
		63.0	Angular	5.60
		86.2	Angular	
		113.0	Angular	
Chase and Draeger [4]	44–180	93.5±3.1	Spherical	4.90
Present work				
Column diameter (10 mm)				
Fractogel HW 55	40–63	51.5	Angular	4.65
LiChroprep DIOL	25–40	32.5	Angular	4.90
LiChroprep DIOL	40–63	51.5	Angular	5.28
Fractosil 1000	63–100	81.5	Angular	4.89

instrumental system used in these studies, and the fact that the adsorbent particles were heterogeneous in terms of their particle diameter, which would result in the larger particles being less affected by the passage of fluid at low flow-rates, resulting in their retention at the bottom of the column, whilst the smaller particles moved upwards, the minimum fluidising velocity of the Fractogel HW55, LiChroprep DIOL (25–40 μm) and LiChroprep DIOL (40–63 μm) were determined using the correlations proposed either by Wen and Yu [34] or by Kunii and Levenspiel [66]. The derived values indicated that a very low linear flow-rate was required to cause the particles to be in the loosest form of packing. For example, from the correlations proposed by Wen and Yu [34] and Kunii and Levenspiel [66], the minimum velocity required to cause a bed containing Fractogel HW55 and LiChroprep DIOL (25–40 μm) to be in the loosest form of packing was 0.002 cm min^{-1} and 0.08 cm min^{-1}, respectively. Fractogel

Table 2
Experimental and theoretical values of the minimum fluidising velocities of different adsorbents

Particle	Experimental (cm/min)[a]	Wen and Yu correlation [34] (cm/min)	Levenspiel [21] correlation (cm/min)
Fractogel HW55 (40–63 μm)	[b]	0.02	0.02
LiChroprep DIOL (25–40 μm)	[b]	0.010	0.011
LiChroprep DIOL (40–63 μm)	[b]	0.03	0.03
Fractosil 1000 (63–100 μm)	0.100	0.08	0.08

[a] Column I.D. = 10 mm.
[b] Accurate experimental values of the minimum fluidising velocity could not be determined by the pressure drop method.

HW55 had the lowest minimum fluidising velocity, followed by LiChroprep DIOL (25–40 μm) and then LiChroprep DIOL (40–63 μm), with Fractosil 1000 exhibiting the highest minimum fluidising velocity. These data are consistent with the expected trends if the density and particle size of these adsorbents are taken into account, i.e. Fractogel HW55 has the lowest density (1.06 g cm^{-3}) while Fractosil 1000 has the highest density (1.35 g cm^{-3}) and the largest particle size.

Table 2 also shows the minimum fluidising velocity of Fractosil 1000 determined by the pressure drop method. The minimum velocity determined by the intersection of the two curves (Fig. 4) was 0.1 cm min^{-1}. The experimental data were higher in value than the values predicted from literature correlations. According to the Wen-Yu correlation, the minimum velocity required to cause the slightest expansion of the bed should be 0.082 cm min^{-1}. This difference between the predicted and experimental values could be due to the manner in which the pressure drop was measured. Since the pressure drop was measured from the bottom of the column, the pressure drop exerted by the distributor (glass beads) was also included and this will result in an overestimate of the value of the minimum fluidisation velocity. When compensation is made for the contribution of the distributor, a value of 0.053 cm min^{-1} was obtained.

Fig. 4 shows the plot of the pressure drop against the superficial velocity in a packed and fluidised column of the same cross-sectional dimensions containing the same quantity of the Fractosil 1000 adsorbent. In the packed column, the pressure drop increased linearly with the superficial velocity, with values ranging from 22 kPa at a superficial velocity of 0.318 cm min^{-1} to 90 kPa at a superficial velocity 1.28 cm min^{-1}. In the fluidised column, a smaller increase in pressure drop was observed over the same linear flow-rate, with the pressure drop at superficial velocities >0.1 cm min^{-1} following a linear trend. As apparent from these results, the general behaviour expected for the pressure drop curve of a fully fluidised column, whereby the initial increase in pressure drop was followed by a plateau value when the column was completely fluidised, was not observed. Above the minimum fluidising velocity, the slope of the pressure drop curve was reduced, but never became zero. This finding indicates that above the minimum fluidising velocity, the pressure drop was still a function of the linear flow-rate. As noted above, this observation could be due to the fact that the column accessories (tubing, distributor, etc.) were contributing to the increase in pressure drop at the higher flow-rates. The effect of these accessories was demonstrated by carrying out the same experiments with the column containing no adsorbent particles. The effect of the column accessories on the pressure drop is shown in Fig. 4, where a pressure drop ranging from 5 to 61 kPa was observed when the superficial velocity was raised from 0.32 to 3.82 cm min^{-1}. Once compensation had been taken into account for these column accessory effects, then the pressure drop profile for the column containing the fluidised particles reached a plateau value at a superficial value of 0.053 cm min^{-1}.

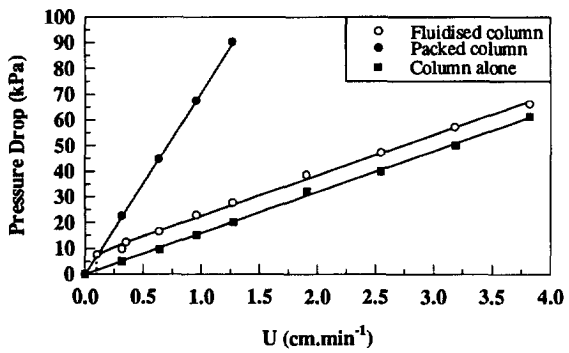

Fig. 4. Effect of the flow-rate on the pressure drop in both the packed and fluidised columns (I.D. 10 mm). Fractosil 1000 (2.5 g) was used as the adsorbent and distilled water was used as the eluent. The static bed height was 3.0 cm.

From the correlations proposed by Wen and Yu [34] and Kunii and Levenspiel [66], the effect of the particle size on the minimum fluidising velocity was determined. The results are shown in Table 2. These results indicate that the minimum fluidising velocity increased with the square of the particle diameter. The data obtained from the above correlations with the silica-based adsorbents were compared with analogous results obtained by Draeger and Chase [1] who used lower density particles (Sepharose Fast Flow, 44–180 μm, 1131 kg m^{-3}). Despite the fact that the minimum fluidising velocity (0.04 cm min^{-1}) employed in this early study with an agarose-based adsorbent was higher than the value obtained

in the present investigation with the silica-based adsorbents, it is noteworthy that at the minimum fluidisation value not all of the Sepharose particles could have been expanded, if the ratio between the smallest and the largest sized particles are taken into account [34,47–49,57,67,68].

3.2.7. Determination of the terminal velocity

The experimental determination of the terminal velocity was achieved from the y-intercept of the plots of the logarithm of the superficial velocity against the log of the bed voidage (Fig. 3). The experimental terminal velocity of the respective adsorbents are shown in Table 3. Fractogel HW55 had the lowest terminal velocity whilst Fractosil 1000 had the highest terminal velocity. For example, the velocity required to elute Fractogel HW55 out of a column of dimensions 1.6×2.6 cm was 0.32 cm min^{-1}, whilst the velocity required to elute Fractosil 1000 out of the column was 12.88 cm min^{-1}. Extrapolation of the plots of the logarithm of the superficial velocity versus bed voidage at a bed voidage equal to one gave the terminal velocity (Fig. 5) for each adsorbent, with parallel lines obtained in each case. Similar results have been obtained [69] with sand particles ranging from 20.2 to 113 mm in diameter fluidised in distilled water. Different results were obtained when the logarithm of the superficial velocity was plotted against the bed voidage, as shown as in Table 4. The extrapolation of the line at $\epsilon = 1$ gave higher values of the terminal velocity. In certain cases, the differences in values were as high

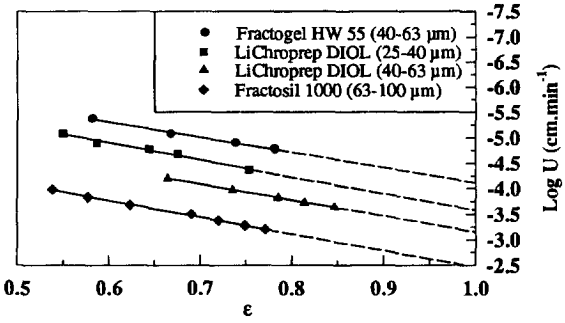

Fig. 5. Plot of the bed voidage versus the logarithm of the superficial velocity for different adsorbents. The column dimensions and eluent composition are given in the legend to Fig. 2.

as three fold, consistent with the fact that the particles had a heterogeneous size distribution.

Comparison of the experimental data obtained from the plots of the logarithm of the superficial velocity against the logarithm of the bed voidage for different chromatographic adsorbents with the corresponding values obtained from Stokes equation and from the correlation proposed by Pinchbeck and Popper [70] revealed that the results were within the same range. In the case of Fractogel HW55, the values obtained by correlations were higher than the experimental data, whilst for LiChroprep DIOL (40–63 μm) and Fractosil 1000 the opposite situation was observed. Except for Fractosil Si1000, where the difference between the experimental data and the theoretical data was higher than 50%, the difference between the theoretical data and the experimental values was around 20%.

Table 3
Experimental and theoretical values of the terminal velocities of different adsorbents

Particle	Experimental (cm/min)		Stokes correlation [26] (cm/min)	Pinchbeck correlation [70] (cm/min)
	Log U vs. Log ϵ	Log U vs. ϵ		
	Column I.D. = 10 mm	Column I.D. = 10 mm		
Fractogel HW 55 (40–63 μm)	0.32	0.46	0.48	0.48
LiChroprep DIOL (25–40 μm)	0.95	2.63	0.99	0.99
LiChroprep DIOL (40–63 μm)	3.33	4.27	2.68	2.67
Fractosil 1000 (63–100 μm)	12.89	20.95	7.59	7.92

Table 4
Experimental and theoretical values of the Reynolds number at the terminal velocities of different adsorbents

Particle	Experimental		Stoke correlation	Pinchbeck correlation [70]
	Log U vs. Log ϵ	Log U vs. ϵ		
	Column I.D. = 10 mm	Column I.D. = 10 mm		
Fractogel HW55 (40–63 μm)	0.03	0.04	0.04	0.04
LiChroprep DIOL (25–40 μm)	0.005	0.01	0.005	0.005
LiChroprep DIOL (40–63 μm)	0.03	0.04	0.02	0.02
Fractosil 1000 (63–100 μm)	0.18	0.29	0.10	0.11

The Reynolds number was also determined to ascertain whether a transition in the fluid flow characteristics occurred inside the column when the flow-rate was increased, i.e. whether a change from a laminar regime to a turbulent regime occurred. Irrespective of the type of particle size used in our experiments, the Reynolds number was less than 0.2 when derived from the plots of the logarithm of the superficial velocity versus the logarithm of the bed voidage (Table 4). Similarly, use of the value of the terminal velocity determined from the correlations based on the Stokes equation or the Pinchbeck and Popper [70] approach, respectively, gave a Reynolds number which was less than 0.2. However, at its terminal velocity, Fractosil 1000 had a Reynolds number that was not far from the threshold value, when the logarithm of the superficial velocity was plotted against the logarithm of the bed voidage. Because of the low density and low particle size, a relatively low flow-rate was required to expel the adsorbents from the column. The fluidisation range for all the adsorbents (the ratio of terminal velocity to the minimum fluidising velocity) was also determined and the values (95–130) were within the same range as that obtained by Pinchbeck and Popper [70] who studied the fluidisation range on ballotini, microspherical alumina, microspherical catalyst and ground silica.

3.2.8. Determination of the dispersion coefficient

Fig. 6 shows the dimensionless output tracer concentration (C/C_0) plotted against the fluid volume applied to the fluidised bed loaded with Fractogel HW55 in a column with the dimensions 26× 1.6 cm, at a superficial velocity of 0.101 cm min^{-1}. Because of the nature of the adsorbent (small particle size and low density), it was impossible to increase the velocity beyond 0.4 cm min^{-1} without moving the adsorbent out of the column. Within the range of flow-rates studied, the theoretical curves derived from the ADM and the TSM fitted the experimental data. The dispersion number (D/U_0L) extracted from the ADM was 0.008, which corresponded to 60 mixing stages from the TSM when using the relationship proposed by Kramers and Alberda [24], i.e. Eq. 12. The derived dispersion coefficient was equal to 0.004 cm^2 min^{-1}. Similar values for the dispersion coefficient have been obtained by Draeger and Chase [1] with low density adsorbents, e.g. Q-Sepharose Fast Flow. The low value of the dispersion

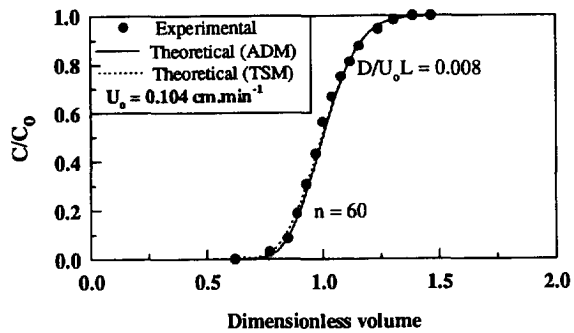

Fig. 6. Comparison of the curve fit of the axial dispersion model (ADM) and the tanks in series model (TSM) to the experimental data. Fractogel HW55 (2.5 g) was packed into a column (I.D. 10 mm) and 0.15 M sodium acetate, pH 4.5, was used as the eluent.

number indicated that the fluid was moving in a plug flow manner in the column.

Since the fluid flow characteristics of the expanded-bed column in these experiments is similar to that obtained in the traditional packed column, performance criteria for a packed column can be applied here. One of these criteria includes determination of the rate at which a protein migrates (and binds) in a conventional packed column. In this case, an important variable parameter will be the effect on bed voidage as the flow-rate is changed. Fig. 7 shows the experimental and predicted breakthrough profiles obtained from the loading of HSA in 0.15 *M* sodium acetate buffer, pH 4.5, onto LiChroprep DIOL (40–63 μm) at a linear flow-rate of 1.4 cm min^{-1}. Compared with the narrow range of flow-rates applied to cause expansion of Fractogel HW55, a wider range of flow-rates was possible to affect expansion of LiChroprep DIOL (40–63 μm), because the adsorbent has a higher density. Fig. 7 shows that a single theoretical breakthrough profile derived from the ADM and TSM could not fit the entire range of experimental data, because a single value of the dispersion coefficient did not prevail. Experimental breakthrough curves were curvilinear, with the theoretical curve having a dispersion number equal to 0.01, matching the lower portion of the experimental data, whilst the theoretical curve having a dispersion number equal to 0.02 matched the upper portion of the experimental breakthrough profile. When the respective dispersion numbers were averaged, a value equal to 0.015 was obtained, resulting in a value for the average dispersion coefficient, derived from the average dispersion number, equal to 0.024 cm^2 min^{-1}. The number of stages that matched the experimental breakthrough was 54 for the lower portion of the curve and 24 for the upper portion of the curve, giving an average number of stages equal to 39. The dispersion number extracted from the average *n* stages using Eq. 12 was within the same range as that obtained from the ADM. Despite having a higher dispersion value than that obtained with Fractogel HW55, the dispersion number for the LiChroprep DIOL (40–63 μm) system was still below the critical value (0.02), and we can conclude that at that particular linear velocity, the flow inside the column was still laminar.

Fig. 8 shows the plot of the dimensionless volume against the ratio of the eluent concentration to the influent concentration in a column containing Fractosil 1000 as the adsorbent and eluted at different

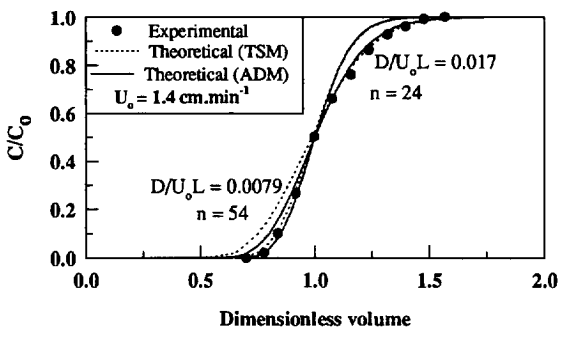

Fig. 7. Comparison of the curve fit of the axial dispersion model (ADM) and the tanks in series model (TSM) to the experimental data. LiChroprep DIOL (2.5 g) was packed into a column (I.D. 10 mm) and 0.15 *M* sodium acetate, pH 4.5, was used as the eluent.

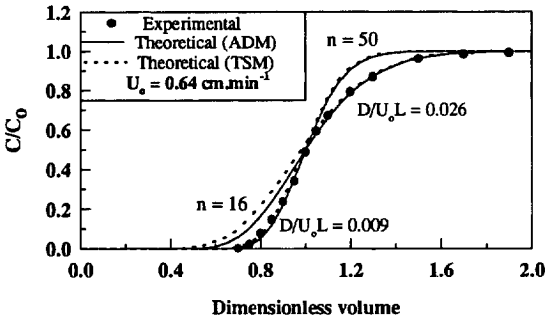

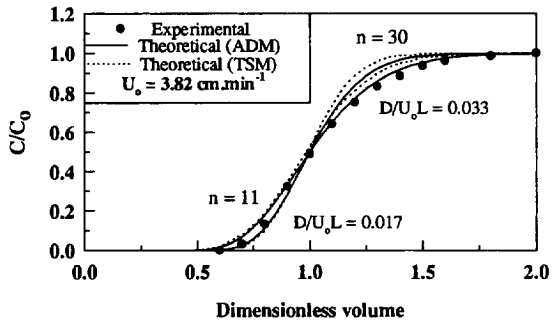

Fig. 8. Comparison of the curve fit of the axial dispersion model (ADM) and the tanks in series model (TSM) to the experimental data for Fractosil 1000 (2.5 g) at different flow-rates in a fluidised column (I.D. 10 mm) with 0.15 *M* sodium acetate, pH 4.5, used as the eluent.

flow-rates. As evident, a single theoretical curve could not be fitted to the experimental data encompassing the different flow regimes. The D/U_oL values and the n-index values which gave the best fit to each curve of the experimental data are presented in Table 5. It was observed that the average dispersion number increased with the linear flow-rate. At an interstitial velocity of 2.06 cm min^{-1}, the average dispersion numbers were 0.018 and 0.013 from the ADM and TSM, respectively. As the interstitial velocity was increased 2.5 fold, the dispersion number increased by 38 and 56%, as derived from the ADM and TSM, respectively. The slight increase in the dispersion number as the superficial velocity was increased could be due to the distance separating the particles from each other. At an interstitial velocity of 2.05 cm min^{-1}, the bed voidage was 0.62 and at an interstitial velocity of 4.95 cm min^{-1}, the bed voidage was 0.77. Greater bed voidage, caused by a reduction in the number of particles occupying a particular space, thus affected the dispersion number in accord with the conclusion of Kramers and Alberda [24].

Fig. 9 shows the plots of the dispersion number and the dispersion coefficient against the interstitial velocity for the Fractosil 1000 adsorbent, utilising data obtained from the ADM and TSM with columns of the same diameter. The dispersion coefficient and dispersion number followed the same trend with changes in the flow-rate. A larger increase in the values of the dispersion coefficient was observed in

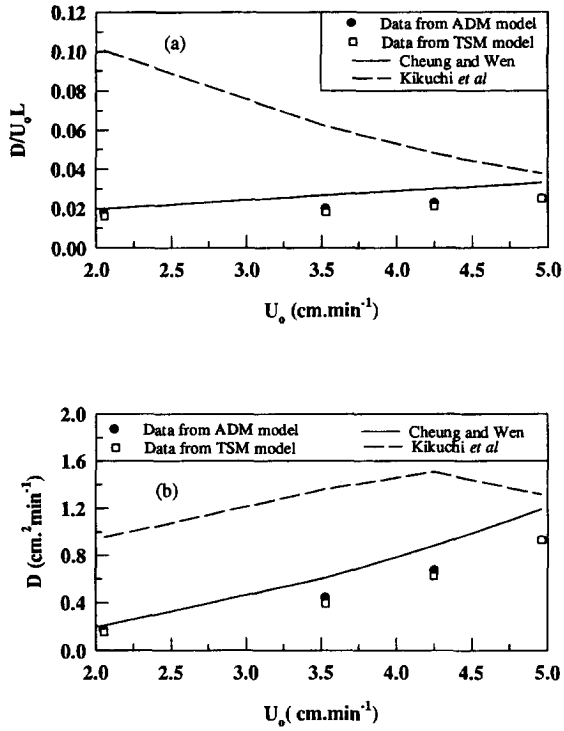

Fig. 9. Determination of the mixing characteristics in the fluidised column. Plot of (a) liquid axial dispersion number and (b) liquid axial dispersion coefficient calculated from the experimental data with the predictions obtained from literature correlations. A well-mixed suspension of Fractosil 1000 (2.5 g) was initially allowed to settle in a column (I.D. 10 mm) containing 0.15 M sodium acetate, pH 4.5, as the buffer and then the same buffer was pumped through at different superficial velocities.

Table 5
Experimental results of the axial dispersion coefficient of different adsorbents

Adsorbent	U_o (cm/min)	Data derived from the ADM [21]			Data derived from the TSM [26]			
Amount used = 2.5 g		D/U_oL	Average	D ($cm^2 min^{-1}$)	n	average	D/U_oL	D (cm^2 min^{-1})
Fractogel HW55	0.10	0.008		0.004	60	60	0.008	0.004
LiChroprep DIOL	1.40	0.01	0.015	0.24	54	39	0.013	0.21
(40–63 μm)		0.02			24			
Fractosil 1000	0.64	0.009	0.018	0.17	50	33	0.016	0.15
(63–100μm)		0.026			16			
	1.28	0.014	0.020	0.44	39	29	0.018	0.39
		0.026			19			
	2.54	0.016	0.023	0.67	36	25	0.021	0.62
		0.030			13			
	3.82	0.016	0.025	0.93	30	21	0.025	0.93
		0.033			11			

the range of flow-rates studied compared to the dispersion number. The experimental data were also compared with the correlation proposed by Kikuchi et al. [17] and Chung and Wen [32]. According to the correlation proposed by Chung and Wen [32], a similar trend is predicted as that obtained in the present investigation but with higher values, whilst the correlation proposed by Kikuchi et al. [17] predicted a decrease in dispersion number in the range of flow-rates studied and a maxima in dispersion coefficient.

4. Conclusions

The present investigations have confirmed that the degree of mixing of fluid inside a column will depend on the design of the column. Poor distributor performance will lead to channelling and this will eventually result in an overestimation of the column performance. Due to the presence of channelling, the particles will move faster in the column and will be detected at the outlet at an earlier stage. The particle diameter and density will contribute to a greater mixing of the fluid inside the column. However, it has been observed that during the adsorption of a solute to an immobilised ligand on a particle having a large diameter, the additional mass transfer resistance of larger particle diameter will limit the choice of the maximum size of the particle that can be used in a specific application. In the present investigations, the degree of mixing of fluid inside the column has been determined by using the tracer method. When the adsorbent has a density which is in the same range as that of the flowing fluid, the degree of mixing is poor and the fluid behaves in a plug flow fashion. Poor liquid mixing was observed when Fractogel HW55 and LiChroprep DIOL were used as adsorbents. The poor liquid mixing was characterised by a low value of the dispersion number and of the dispersion coefficient. The effect of flow-rate on the dispersion coefficient shows that the dispersion coefficient follows the same trend as the flow-rate was increased. However, the predicted profiles obtained from the ADM and the TSM failed to fit the experimental data.

From our results, it was also observed that the minimum fluidising velocity and the terminal velocity were affected by the particle size and particle density. At the terminal velocity, it was observed that the nature of the fluid flow was still laminar when Fractogel HW55, LiChroprep DIOL (25–40 μm) and LiChroprep DIOL (40–63 μm) were packed inside the column. The results indicated that the fluid moved within the column in a plug flow manner. Only Fractosil 1000 exhibited a Reynolds number in the range of the threshold value (0.2). As a result of this observation, adsorbents based on Fractosil 1000 would appear to be suitable candidates for use in expanded-bed/fluidised columns. Experimental results obtained with associated studies carried out in this laboratory with immobilised heparin–Fractosil adsorbents have confirmed this conclusion [9].

The experiments performed with the prototype columns have shown that they are reliable for fluidisation experiments, since the expansion characteristics were within the same range as those predicted by the Richardson-Zaki correlation. Experiments performed with the fluidised column have shown that high flow-rates can be applied without a large change in the pressure drop and good liquid mixing can be achieved if an appropriate high density adsorbent is used. The application of these expanded-bed/fluidised column systems should prove to be advantageous in studies on the adsorption of proteins.

5. List of symbols

C/C_o = dimensionless concentration.
d_p = particle diameter (m).
D = dispersion coefficient (m^2 s).
D/U_oL = dispersion number.
D_a = axial diffusivity.
D_e = effective diffusivity (m^2 s^{-1}).
erf = error function in Eq. 10.
g = acceleration due to gravity (m s^{-2}).
L = bed height at any flow-rate (m).
L_o = bed height when particles are at rest (cm).
n = expansion index.
m = number of tanks in Eq. 11.
Re = particle Reynolds number at a specified flow-rate (d_p ρ_f U/υ).
Re_{mf} = particle Reynolds number on the onset of fluidisation (d_p ρ_f U_{mf}/υ).

Re_t = particle Reynolds number at the terminal velocity ($d_p\ \rho_f\ U_t/\nu$).
t = time (s).
U = superficial velocity (cm min^{-1}).
U_o = interstitial velocity (cm min^{-1}).
U_t = terminal velocity (cm min^{-1}).
Y = Re_{mf}/Re
z = $(U_o t+\chi)/L$

6. Greek symbols

$1-\epsilon$ = the fraction solid at height L.
ϵ = bed voidage.
ϵ_{mf} = column bed voidage when particles are at rest.
l = kinematic viscosity ($m^2\ s^{-1}$)
θ = $t/\bar{t}$
ρ_s = density of solid (kg m^3).
ρ_f = density of fluid (kg m^3).
χ = characteristic length.
Ω = energy dissipation rate ($m^2\ s^{-3}$).
ν = viscosity (kg m^{-1} s)

Acknowledgments

These investigations were supported by a grant from the Australian Research Council. The award of the Alexander von Humboldtforschungspreis to Milton T.W. Hearn is gratefully acknowledged.

References

[1] N.M. Draeger and H.A. Chase, Int. Chem. Eng. Symp. Ser., 118 (1990) 161.
[2] N.M. Draeger and H.A. Chase, Trans. Inst. Chem. Eng., 69 (1991) 45.
[3] N.M. Draeger and H.A. Chase, Bioseparation, 2 (1991) 67.
[4] H.A. Chase and N.M. Draeger, J. Chromatogr., 597 (1992) 129.
[5] G.E. McCreath, H.A. Chase, D.R. Purvis and C.R. Lowe, J. Chromatogr., 597 (1992) 189.
[6] G.E. McCreath, H.A. Chase and C.R. Lowe, J. Chromatogr. A, 659 (1994) 275.
[7] M. Hansson, S. Stahl, R. Hjorth, M. Uhlen and T. Moks, BioTechnology, 12 (1994) 285.
[8] J. Thommes, M. Halfar, S. Lenz and M.-R. Kula, Biotechnol. Bioeng., 45 (1995) 205.
[9] M. Bjorklund and M.T.W. Hearn, J. Chromatogr. A, (1996) in press.
[10] T.J. Hanratty, G.A. Latinen and R.H. Wilhelm, AIChE J., 2 (1956) 372.
[11] D. Handley, A. Doraisamy, K.L. Butcher and N.L. Franklin, Trans. Inst. Chem. Eng., 44 (1966) 260.
[12] C.R. Carlos and J.F. Richardson, Chem. Eng. Sci., 23 (1968) 813.
[13] L.D. Ryan and C.S. Vestling, Arch. Biochem. Biophys., 160 (1974) 279.
[14] A. Kmieck, Chem. Eng. J., 15 (1978) 1.
[15] M. Asif, N. Kalogerakis and L.A. Behie, Chem. Eng. J., 49 (1992) 17.
[16] M. Asif, N. Kalogerakis and L.A. Behie, AIChE J., 37 (1991) 1825.
[17] K.I. Kikuchi, H. Konno, S. Kakutani, T. Sugawara and H. Ohashi, J. Chem. Eng. Japan, 17 (1984) 362.
[18] A. Bascoul, J.P. Riba, C. Alran and J.P. Couderc, Chem. Eng. J., 38 (1988) 69.
[19] W.T. Tang and L.S. Fan, Chem. Eng. Sci., 45 (1990) 543.
[20] X. Zhao, Y. Wang and T. Hu, Fluidisation 1991, 4th China–Japan Symp., Academia Sinica, Beijing, China, 1991, p. 346.
[21] O. Levenspiel, Chemical Reactor Engineering, Wiley, 2nd ed., 1972.
[22] R.B. McMullin and M. Weber, Trans. Am. Inst. Chem. Engrs., 31 (1935) 409.
[23] K. Schoenemann, Dechema Monogr., 21 (1952) 203.
[24] H. Kramers and G. Alberda, Chem. Eng. Sci., 2 (1953) 173.
[25] A. Klinkerberg and H.H. Sjenitzer, Chem. Eng. Prog., 44 (1956) 17.
[26] Q.M. Mao and M.T.W. Hearn, Biotechnol. Bioeng. (1995) in press.
[27] R.H. Wilhelm and M. Kwauk, Chem. Eng. Prog., 44 (1948) 201.
[28] G. Narsimham, AIChE J., 11 (1965) 550.
[29] U.P. Ganguly, Can. J. Chem. Eng., 58 (1980) 559.
[30] K.V.K. Rao and S.G. Pakash, Can. J. Chem. Eng., 60 (1982) 859.
[31] C. Webb, G.M. Black and B. Atkinson, Chem. Eng. Res., 61 (1983) 125.
[32] S.F. Chung and C.Y. Wen, AIChE J., 14 (1968) 857.
[33] C.Y. Wen and L.S. Fan, Can. J. Chem. Eng., 52 (1974) 673.
[34] C.Y. Wen and Y.H. Yu, AIChE J., 12 (1966) 610.
[35] C.Y. Wen and L.S. Fan, Chem. Eng. Sci., 28 (1973) 1768.
[36] P.R. Krishnaswamy and L.W. Shemilt, Can. J. Chem. Eng., 50 (1972) 419.
[37] P.R. Krishnaswamy, R. Ganapathy and L.W. Shemilt, Can. J. Chem. Eng., 56 (1978) 550.
[38] S.G. Mehta and L.W. Shemilt, Can. J. Chem. Eng., 54 (1976) 43.
[39] E.J. Cairns and J.M. Praunitz, AIChE J., 6 (1960) 400.
[40] I. Muchi, T. Harumo and K. Sasaki, Kagaku Kogadu, 25 (1961) 747.
[41] C. Bruinzeel, C.H. Reman and E.Th. Vander Laan, Proc. Symp. Interact. Fluids, Inst. of Chem. Engrs., London, 1962, p. 120.
[42] S.C. Kennedy and R.H. Bretton, AIChE J., 12 (1966) 24.

[43] I.M. Stayanovskii, J. Appl. Chem. USSR, 34 (1961) 109.
[44] U. Aoyama, K. Ogushi, K. Koida and H.J. Kaboku, J. Chem., Eng. Jpn., 1 (1967) 158.
[45] M.L. Michelsen and K. Ostergaad, Chem. Eng. J., 1 (1970) 37.
[46] Y. Kato, A. Mishiwaki, T. Fukua and S. Tanaka, J. Chem. Eng. Jpn., 5 (1972) 112.
[47] A.P. van der Meer, C.M.R.J.P. Blanchard and J.A. Wesselingh, Chem. Eng. Res. Des., 62 (1984) 214.
[48] A.K.A. Juma and J.F. Richardson, Chem. Eng. Sci., 38 (1983) 955.
[49] M.R. Al-Dibouni and J. Garside, Trans. Inst. Chem. Engrs., 57 (1979) 94.
[50] B.K. Dutta, S. Bhattacharya, S.K. Chaudhury and B. Barman, Can. J. Chem. Eng., 66 (1988) 676.
[51] H. Kramers, M.D. Westermann, J.H. De Groot and K.A.A. Dupont, 3rd Congress European Federation; Chem. Eng. Proc. Symp., (1962) 114.
[52] S.A. El-Temtamy, Y.O. El-Sharnoubi and M.M. El-Halwagi, Chem. Eng. J., 18 (1979) 151.
[53] S.D. Kim, C.G.J. Baker and M.A. Bergougnou, Can. J. Chem. Eng., 50 (1976) 695.
[54] A.N. Emery and J.P. Cordoso, Biotechnol. Bioeng., 20 (1978) 1903.
[55] R. Lekan and J.G. Elgin, Chem. Eng. J., 3 (1972) 136.
[56] B.K. Pathak, V.N. Singh and P.C. Singh, Indian J. Technol., 17 (1979) 247.
[57] J.B. Joshi, Chem. Eng. Res. Des., 61 (1983) 143.
[58] L.J. Tichateck, C.H. Barkelew and T. Baron, AIChE J., 3 (1957) 439.
[59] J. Benarek and I. Klumpar, Collect. Czech. Chem. Commun., 23 (1958) 1.
[60] C. Metzdorf, P.F. Fauquex, E. Flashel and X. Renken, Ger. Chem. Engr., 6 (1985) 358.
[61] J.F. Richardson and X. Zaki, Trans. Inst. Chem. Engrs., 32 (1954) 35.
[62] J.F. Richardson and R.A. Meikle, Trans. Inst. Chem. Engrs., 39 (1961) 348.
[63] L.G. Gibilaro, R. di Felice, P.U. Foscolo and S.P. Waldram, Chem. Eng., 37 (1988) 25.
[64] A. Chianese, G. Frances, F. DiBerardino and L. Bruno, Chem. Eng. J., 50 (1992) 87.
[65] R.L. Whitmore, J. Inst. Fuel., 30 (1957) 328.
[66] D. Kunii and O. Levenspiel, Fluidization Engineering, Wiley, New York, 1969, pp. 72–79.
[67] R.F. Hoffmann, L. Lapidus and J.C. Elgin, AIChE J., 6 (1960) 321.
[68] B.L.A. Martin, Ph.D. Thesis, University of Strasbourg, 1979.
[69] R. Jottrand, J. Appl. Chem., 2 (1952) S17.
[70] P.H. Pinchbeck and F. Popper, Chem. Eng. Sci., 6 (1956) 57.
[71] H.J Wirth and M.T.W. Hearn, J. Isolation Purif., (1995) in press.